

# RAMAN MICROSCOPE AND QUANTUM YIELD STUDIES ON THE PRIMARY PHOTOCHEMISTRY OF A<sub>2</sub>-VISUAL PIGMENTS:

BRIDGETTE BARRY,\*RICHARD A. MATHIES,\* JOHANNES A. PARDOEN,<sup>‡</sup> AND JOHAN LUGTENBURG<sup>‡</sup>

\*Department of Chemistry, University of California, Berkeley, California 94720; and <sup>‡</sup>Department of Chemistry, Leiden University, 2300 RA Leiden, The Netherlands

**ABSTRACT** The 77-K resonance Raman vibrational spectrum of intact goldfish rod photoreceptors containing 3,4-dehydro (A<sub>2</sub>) retinal is dominated by scattering from the 9-*cis* component of the steady state at all excitation wavelengths. Intact goldfish photoreceptors were regenerated with an A<sub>1</sub>-retinal chromophore to determine whether this behavior is caused by the protein or the chromophore. The resulting Raman spectrum was typical of an A<sub>1</sub>-pigment exhibiting significant scattering from all three components of the steady state: rhodopsin, bathorhodopsin, and isorhodopsin. Furthermore, regeneration of bovine opsin with A<sub>2</sub>-retinal produces a characteristic "A<sub>2</sub>-Raman spectrum" that is dominated by scattering from the 9-*cis* pigment. We conclude that the differences between the Raman spectra of the A<sub>1</sub>- and A<sub>2</sub>-pigments are caused by some intrinsic difference in the photochemical properties of the retinal chromophores. To quantitate these observations, the 77-K absorption spectra and the photochemical quantum yields ( $\phi$ ) of the native A<sub>2</sub>-goldfish and the regenerated A<sub>2</sub>-bovine pigments were measured. In the goldfish A<sub>2</sub>-pigment, the value of  $\phi_4(9\text{-}cis \rightarrow trans)$  is 0.05;  $\phi_3(trans \rightarrow 9\text{-}cis)$  is 0.10; and  $\phi_2(trans \rightarrow 11\text{-}cis)$  is 0.35. By contrast, in the bovine A<sub>1</sub>-pigment, these quantum yields are 0.10, 0.053, and 0.50, respectively. The reduced value of  $\phi_4$  and the increased value of  $\phi_3$  in the goldfish pigment confirms that the 9-*cis* isomer is photochemically more stable in A<sub>2</sub>-pigments.

## INTRODUCTION

Vision in vertebrates begins with the absorption of a photon by rhodopsin in the photoreceptor cells of the retina (1). Rhodopsin contains an 11-*cis* retinal (A<sub>1</sub>-pigment) or an 11-*cis*-3,4-dehydroretinal chromophore (A<sub>2</sub>-pigment). In both pigments, the chromophore is covalently bound to a lysine residue of the protein, opsin, as a protonated Schiff base. Absorption of a photon causes an isomerization of rhodopsin's 11-*cis* chromophore to a twisted, all-*trans* configuration in the photoproduct, bathorhodopsin (2–4). Bathorhodopsin decays through a series of intermediates leading to the detachment of all-*trans* retinal from the protein. The meta II intermediate activates a series of enzymes in a "cyclic nucleotide cascade" that cause the lowering of the cGMP level in the cytoplasm and the closure of Na<sup>+</sup> channels in the plasma membrane (5, 6).

The photoproducts of visual pigments can be trapped in a photostationary steady-state mixture at 77 K (7). This mixture contains a 9-*cis* pigment (isorhodopsin), as well as 11-*cis* rhodopsin and the all-*trans* photoproduct (batho-

rhodopsin). Since the components of the steady state have different absorption maxima, the composition of the steady state depends on the wavelength of illumination. The composition of this steady state for the A<sub>1</sub>-bovine pigment has been determined at a range of irradiation wavelengths (3, 8). This information, along with the low-temperature absorption spectra of each intermediate, has been used to determine the isomerization quantum yields at low temperature (8) and to deduce information about the dynamics of photoisomerization (9).

Resonance Raman spectroscopy is a useful technique for studying chromophore structure in visual pigments because the vibrational modes of the chromophore are selectively enhanced by use of a laser wavelength within the absorption band of the pigment (10), and because vibrations of the chromophore are sensitive to the details of chromophore geometry and environment (11). In our Raman studies of A<sub>2</sub>-pigments, we have used a resonance Raman microscope system (12, 13). With this instrument vibrational spectra have been obtained from intact goldfish photoreceptors which contain an A<sub>2</sub>-chromophore absorbing maximally at 522 nm. In contrast to previous studies of A<sub>1</sub>-pigments, we found that the A<sub>2</sub>-pigment spectra were dominated by scattering from the 9-*cis* pigment at all probe wavelengths.

This paper describes Raman microscope and quantum

Dr. Barry's present address is Michigan State University-Department of Energy Plant Research Laboratory/Chemistry Department, Michigan State University, East Lansing, MI 48824.

Correspondence should be addressed to Dr. Mathies.

yield measurements we have performed to understand this observation. First, procedures were developed to bleach and regenerate the pigment inside intact photoreceptors. By studying the goldfish pigment regenerated with A<sub>1</sub>-retinal and bovine rod pigments regenerated with A<sub>2</sub>-retinal, we found that the unexpected steady-state composition of the goldfish A<sub>2</sub>-pigment was an intrinsic property of the A<sub>2</sub>-chromophore. We then analyzed the 77-K steady-state compositions of the A<sub>2</sub>-bovine and A<sub>2</sub>-goldfish pigments to determine photochemical quantum yields. These quantum yield results provide a quantitative understanding of the composition differences between the A<sub>1</sub>- and A<sub>2</sub>-steady states.

## MATERIALS AND METHODS

### Resonance Raman Microscopy

The design and operation of the Raman microscope and cold stage have been described previously (12, 13). Briefly, the photoreceptors are frozen on a 77-K cold stage, and the probing laser beam is focused onto the outer segment by a long working length objective. Raman scattered light is collected by the objective and dispersed onto a multichannel detector.

Goldfish photoreceptor cells were isolated for Raman microscopy by the following procedure. After dark-adapting for 2–12 h, the spinal column of the fish was severed and pithed, and the eyes were removed and hemisected. The retina was detached from the eyecup with a stream of teost Ringer's buffer: 100 mM NaCl, 2.5 mM KCl, 1.0 mM MgCl<sub>2</sub>, 0.5 mM NaH<sub>2</sub>PO<sub>4</sub>, 5.0 mM NaHCO<sub>3</sub>, 10 mM Hepes, pH 7.4 (14). A small piece of the retina was transferred to the sapphire window of the cold stage, where it was immersed in a drop of solution (1 part glycerol mixed with 2 parts 40% [wt/vol] aqueous sucrose) that would form a clear glass at 77 K. The retina was then minced, and the suspension of photoreceptor cells was cooled to liquid nitrogen temperature. All operations were performed under dim red lights.

Our procedure for bleaching the goldfish rod photoreceptors and regenerating them with an A<sub>1</sub>-chromophore was modeled after the protocols in references 15–17. A piece of the goldfish retina in Ringer's was bleached with yellow light for 10 min. This buffer also contained 100 μg/ml of 11-*cis* A<sub>1</sub>-retinal, which helped to preserve cellular morphology. An additional aliquot of retinal in ethanol was then added to raise the concentration by 100 μg/ml. After regenerating for 45 min, the retina was transferred to a 2% bovine serum albumin-Ringer's solution that contained no retinal. Soaking in this solution for 5 min reduced the nonspecific binding of retinal to cellular membranes.

### Preparation of Detergent-solubilized Pigments

To perform absorption and quantum yield measurements on the A<sub>2</sub>-pigments it was necessary to prepare detergent-solubilized samples. Goldfish rod outer segments were isolated on discontinuous sucrose gradients (18) and solubilized in 1% octyl-glucoside on the morning of the experiment. All pigment-detergent solutions were maintained below 4°C at all times. Final pigment concentrations in 1% octyl-glucoside were 0.05 optical density (OD) units per cm. The solubilized pigment had an absorption maximum of 520 nm, which is close to the *in situ* value of 522 nm (19).

For comparison the Raman, absorption, and quantum yield measurements were also performed on bovine rod pigments regenerated with A<sub>2</sub>-retinal. The protocol for isolation of bovine rod outer segments can be found in reference 20. Bovine rod outer segments were lysed, bleached in the presence of NH<sub>2</sub>OH (pH 7), washed, and regenerated with 9-*cis*- or 11-*cis*-3,4-dehydroretinal. The regenerated A<sub>2</sub>-bovine pigment was solubilized in 3% octyl-glucoside and purified using hydroxyapatite chroma-

tography in 1% octyl-glucoside. The pigment samples were concentrated for Raman spectroscopy using centrifuge cones (CF25; Amicon Corp., Danvers, MA). The absorption maximum of the 9-*cis* A<sub>2</sub>-pigment was 500 nm, and the absorption maximum of the 11-*cis* A<sub>2</sub>-pigment was 518 nm.

### Determination of Quantum Yields

The quantum yields for the interconversion of rhodopsin, bathorhodopsin, and isorhodopsin at 77 K are defined according to Suzuki and Callender (8):



The ratios of the quantum yields can be determined by knowing the relative extinctions and steady-state compositions of the three species.

$$\frac{\phi_1}{\phi_2} = \frac{\epsilon_B [\text{Batho}]}{\epsilon_R [\text{Rho}]} \quad \frac{\phi_3}{\phi_4} = \frac{\epsilon_I [\text{Iso}]}{\epsilon_B [\text{Batho}]} \quad (1)$$

The individual quantum yields can then be determined by measuring or knowing  $\phi_1$  and  $\phi_2/\phi_3$ .

The 77-K absorption spectra of solubilized A<sub>2</sub>-pigments were obtained by the method of Yoshizawa (7). The rhodopsin spectrum was recorded after simply cooling the sample in 66% (vol/vol) glycerol, 60 mM NH<sub>2</sub>OH, pH 7 buffer. Illumination from the side with a 476-nm laser beam produced a bathorhodopsin-rich steady-state. The 476-nm steady state was then irradiated at 647 nm to give a pure isorhodopsin spectrum. A pure bathorhodopsin spectrum was obtained by subtracting the appropriately weighted (see below) rhodopsin and isorhodopsin spectra from the 476-nm spectrum. Absorbance studies on the goldfish pigment were performed on a Cary 14 (Varian Associates, Inc., Palo Alto, CA). Studies on the A<sub>2</sub>-bovine pigment were performed on an Aminco DW2-C (SLM Instruments, Inc., Urbana, IL) in dual-wavelength mode.

For the composition experiments, the pigment sample (1% octyl-glucoside-phosphate buffer, 60 mM NH<sub>2</sub>OH, pH 7) was frozen at 77 K and the pigment irradiated with a 100–200 mW, expanded laser beam for 1 h. This produces a steady-state mixture of bathorhodopsin, isorhodopsin, and rhodopsin. Warming the sample in the dark then results in the decay of bathorhodopsin. A room temperature absorption spectrum was recorded and the contributions of rhodopsin and isorhodopsin were determined by a multiple regression fit using pure room temperature rhodopsin and isorhodopsin spectra, and a background spectrum obtained by fully bleaching the sample. The fit was performed between 480 and 700 nm. The amount of the photoproduct produced at each irradiation wavelength was determined by assuming that the total amount of rhodopsin, isorhodopsin, and bathorhodopsin summed to 100%, after correction for the ~3% loss of pigment caused by freezing and thawing. Spectra were recorded on an Aminco DW2-C spectrophotometer. The absorbance at the  $\lambda_{\text{max}}$  of a typical sample of the goldfish pigment was 0.04 OD; the absorbance of the regenerated A<sub>2</sub>-bovine pigment was 0.02 OD.

### Synthesis of A<sub>2</sub>-Retinals

1 g of *n*-bromosuccinimide was added to 1 g of commercial A<sub>1</sub>-retinal dissolved in chloroform at 0°C (21). After 20 min the extent of the reaction was checked by thin-layer chromatography, and if the reaction was complete, 1 g of 1,8-diazabicyclo-undec-7-ene was added. This solution was refluxed for 1.5 h at 61°C. The reaction mixture was then poured into 1 N aqueous HCl. The layers were separated, and the product was purified by column chromatography on silica (10% ether/90% petroleum ether). The yield of all-*trans* A<sub>2</sub>-retinal was 10%. The product was purified further by high performance liquid chromatography in 20% ether/80% pentane. To make the A<sub>2</sub>-retinal isomers, the all-*trans* A<sub>2</sub>-retinal was irradiated for 90 min in acetonitrile with a tungsten lamp. The

isomers were separated by high performance liquid chromatography (22) and were characterized by absorption and mass spectroscopy and by nuclear magnetic resonance. The absorption maxima of the  $A_2$ -retinal isomers were: all-*trans*, 395 nm; 13-*cis*, 385 nm; 11-*cis*, 392, 314, 250 nm; 9-*cis*, 392, 314 nm; 7-*cis*, 378 nm.

## RESULTS

### Resonance Raman Studies

In Fig. 1 we present resonance Raman microscope data on the  $A_2$ -rod photoreceptor cells of the goldfish ( $\lambda_{\max} = 522$  nm; 19). The frequencies and relative intensities of most of the lines in the 1,100–1,300  $\text{cm}^{-1}$  fingerprint region were qualitatively unchanged by variation of the laser probe wavelength from 515 to 583 nm. Experiments with probe wavelengths as blue as 476 nm and as red as 600 nm give similar results (24). Lines in the 1,100–1,300  $\text{cm}^{-1}$  fingerprint region of the spectrum are known to be characteristic of chromophore configuration in  $A_1$ -visual pigments and in  $A_1$ - and  $A_2$ -protonate, Schiff bases (11, 23, 24). The fingerprint regions of spectra *A* and *B* in Fig. 1 bear a marked resemblance to the fingerprint of the 9-*cis*-3,4-dehydroreti-

nal protonated Schiff base (Fig. 1 *C*). The  $\sim 1,512$   $\text{cm}^{-1}$  line in spectra *A* and *B* has been assigned to the ethylenic band of a red-shifted photoproduct (12); however, the weak intensity of this line suggests that this species makes only a small contribution to the scattering in other regions of the spectrum.

This behavior contrasts sharply with the behavior of  $A_1$ -pigments under similar illumination conditions. The Raman spectra of  $A_1$ -pigments obtained with blue and red probe wavelengths are markedly different from each other. The Raman spectrum of the bovine  $A_1$ -pigment obtained with 568-nm excitation has a fingerprint identical to that of the 9-*cis* model compound (3). This is expected since the 568-nm steady state is composed primarily of isorhodopsin. However, the fingerprint of the 514.5-nm spectrum is more complex, because the steady-state mixture contains significant amounts of rhodopsin (31%), isorhodopsin (24%), and bathorhodopsin (45%) (8).

This difference between  $A_1$ - and  $A_2$ -pigments could be caused by the chemical differences between the  $A_1$ - and  $A_2$ -chromophores or by sequence differences between the goldfish and bovine rod opsins. To differentiate between these two possibilities, regeneration experiments were performed on intact goldfish rod photoreceptors and on bovine outer segments. We replaced the 3,4-dehydroretinal chromophore of the goldfish pigment with  $A_1$ -retinal, creating

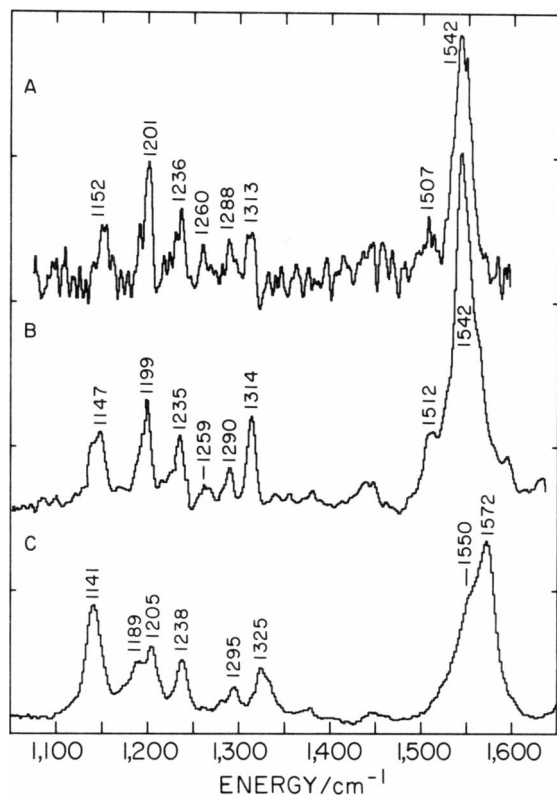


FIGURE 1 (*A* and *B*) Resonance Raman microscope spectra recorded at 77 K, of individual rod photoreceptors from the goldfish, *Carassius auratus*. This photoreceptor contains an  $A_2$ -pigment with an absorption maximum at 522 nm (19). Spectrum *A* was obtained at 583 nm (5 mW), and spectrum *B* was obtained at 514.5 nm (5 mW). (*C*) Resonance Raman spectrum of the *n*-butylamine protonated Schiff base of 9-*cis*  $A_2$ -retinal in carbon tetrachloride. The spectrum was obtained using 752-nm irradiation (90 mW) and a stationary sample; the spectral slit width was 4  $\text{cm}^{-1}$ .

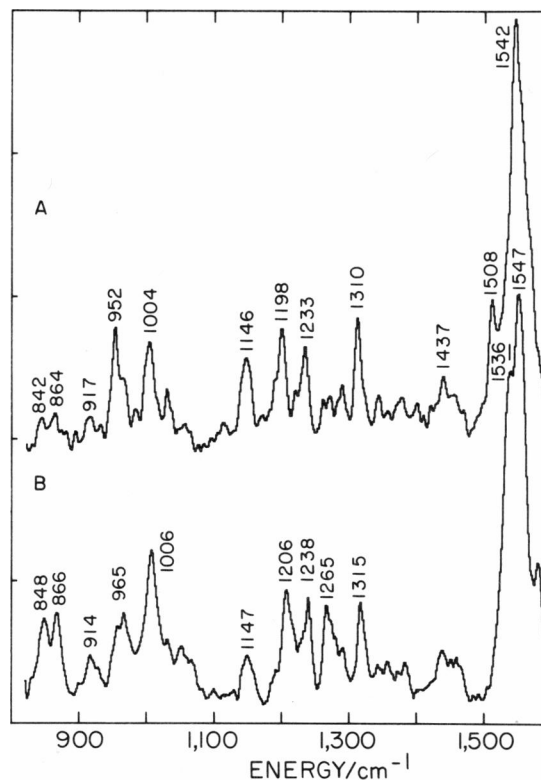


FIGURE 2 Resonance Raman microscope spectra of goldfish rod photoreceptors. (*A*) Spectrum of the native  $A_2$ -pigment (2.5 mW, 488 nm). (*B*) Spectrum of a goldfish rod after regeneration with 9-*cis*  $A_1$ -retinal (5.5 mW, 488 nm).

a regenerated  $A_1$ -goldfish pigment. Fig. 2 presents the Raman microscope spectrum of the regenerated  $A_1$ -goldfish pigment along with the native  $A_2$ -spectrum. The Raman spectrum that is produced by regeneration of bovine opsin with the 9-*cis*  $A_2$ -chromophore is compared with the native  $A_1$ -spectrum in Fig. 3. Notice that the spectrum of the regenerated  $A_1$ -goldfish pigment is very similar to the 488-nm spectrum of the  $A_1$ -bovine pigment shown in Fig. 3 *A*. Particularly striking is the presence of intense lines at 1,536, 848, 866, and 914  $\text{cm}^{-1}$ . The analogous lines in the  $A_1$ -bovine spectrum have been assigned to bathorhodopsin (3, 4). Thus, the contribution that the photoproduct makes to the Raman spectrum increases when the goldfish rod pigment is regenerated with the  $A_1$ -chromophore. Furthermore, Fig. 3 *B* shows that substitution of the  $A_2$ -chromophore into bovine opsin has produced the characteristic 488-nm Raman spectrum of the  $A_2$ -pigment, which is dominated by scattering from the 9-*cis* species. We conclude that the differences we have observed between the Raman spectra of the  $A_2$ - and  $A_1$ -pigments depend primarily on the presence of the 3,4-dehydroretinal chromophore in the binding pocket of the pigment.

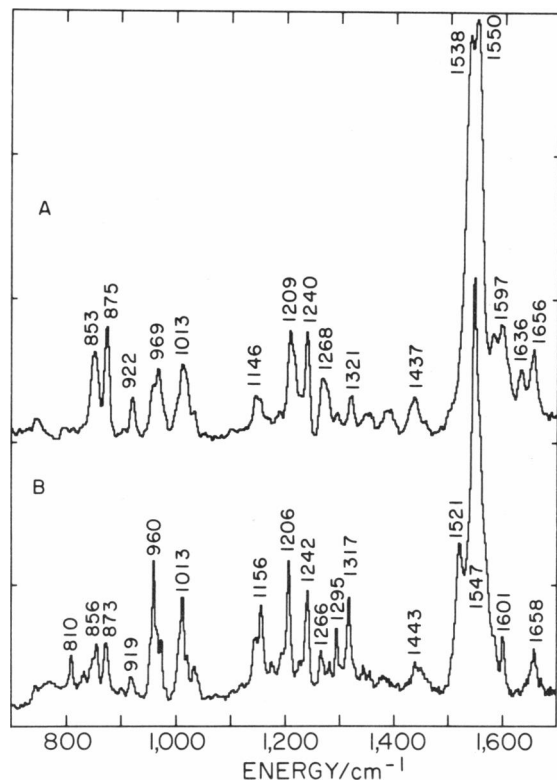


FIGURE 3 Resonance Raman spectra of solubilized bovine rod visual pigments recorded at 77 K. (*A*) Spectrum of the native  $A_1$ -bovine pigment from reference 26 (488-nm probe). (*B*) Spectrum of the bovine pigment after regeneration with 9-*cis* 3,4-dehydroretinal. This spectrum was obtained with a photon-counting Raman system using a 488-nm probe (50 mW) and a slit width of 4  $\text{cm}^{-1}$ .

To obtain a pure spectrum of bovine  $A_2$ -bathorhodopsin to compare with the spectrum of the  $A_1$ -bathorhodopsin, a yellow probe/blue pump experiment was performed using the spinning cell technique developed by Braiman and Mathies (25). Fig. 4 *A* was taken with a 568-nm probe beam alone. When a 488-nm pump is added to the steady state, spectrum 4 *B* is obtained. The blue pump beam will increase the relative amount of bathorhodopsin in the steady state. Our composition measurements show (see below) that the 488 nm + 568 nm steady states contain mainly bathorhodopsin and isorhodopsin. The large increase in intensity at 1,519, 920, 873, and 859  $\text{cm}^{-1}$  argues that these lines are vibrations of a red-shifted photoproduct. When spectrum 4 *A* is subtracted from 4 *B*, we obtain the spectrum shown in *C*, which contains primarily scattering from bathorhodopsin. Spectrum 4 *C* is very similar to the spectrum of native  $A_1$ -bathorhodopsin obtained by Eyring et al. (26).  $A_2$ -bathorhodopsin has an ethylenic stretch at lower frequency than that of  $A_1$ -bathorhodopsin. This difference is consistent with the more red-shifted absorption spectrum of the  $A_2$ -photoproduct

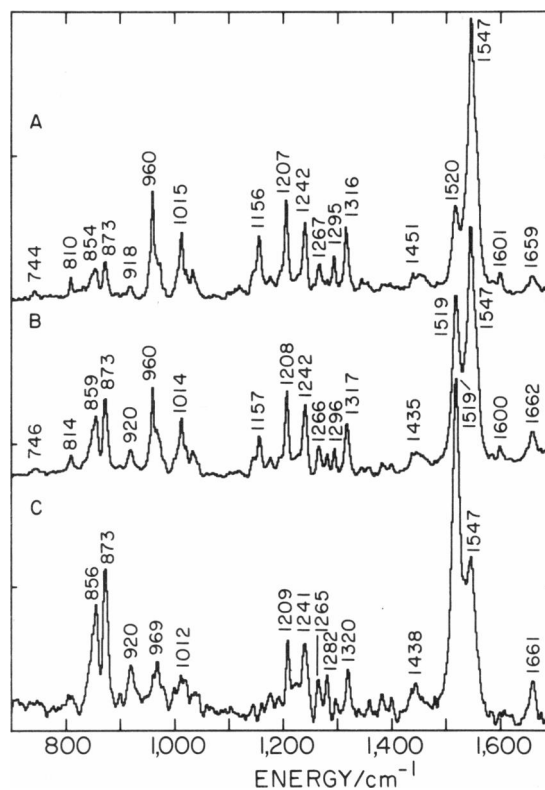


FIGURE 4 Resonance Raman spectra of bovine pigments regenerated with 9-*cis* 3,4-dehydroretinal. These data were obtained using a 77 K spinning cell technique (25). (*A*) Spectrum obtained using a single probe laser at 568 nm (15 mW). (*B*) Spectrum obtained using a probe beam at 568 nm (5 mW) and a spatially displaced, unfocused 250-mW, 488-nm pump. Spectrum *C* was obtained by subtracting *A* from *B* until a flat background was obtained in regions where only spectrum *A* had Raman lines. In all cases, the spectral slit width was 4  $\text{cm}^{-1}$ .

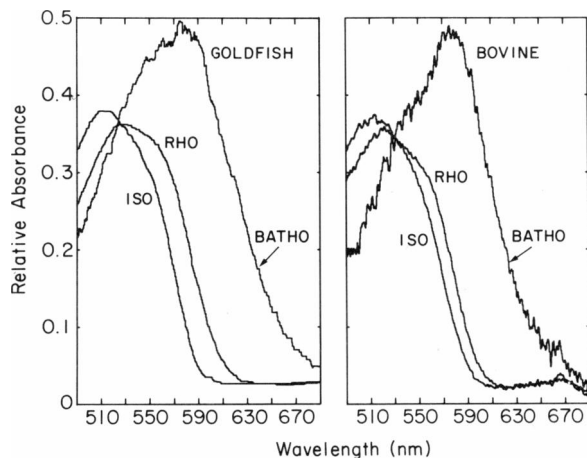


FIGURE 5 Absorption spectra of rhodopsin, isorhodopsin, and bathorhodopsin in the 77-K steady state of the goldfish  $A_2$ -pigment and the regenerated  $A_2$ -bovine pigment.

(see below).  $A_2$ -bathorhodopsin has three enhanced low frequency modes at 856, 873, and 920  $\text{cm}^{-1}$  that are similar in frequency and relative intensity to lines in the  $A_1$ -spectrum (Fig. 3 A).

### Composition and Low-Temperature Absorption Studies

To understand the nature of the photochemical differences between  $A_1$ - and  $A_2$ -pigments, we performed low-temperature absorption and composition studies. Our absorption results (Fig. 5) are in agreement with Yoshizawa's previous work on the carp  $A_2$ -pigment (7). At 77 K, both the  $A_2$ -goldfish and  $A_2$ -bovine pigments form a 9-*cis* compound with an absorption maximum at 515 nm and a photoproduct with an absorption maximum at 580 nm. The  $A_2$ -goldfish rhodopsin has an absorption maximum at 530 nm at 77 K, whereas the regenerated  $A_2$ -bovine rhodopsin at 77 K absorbs maximally at 522 nm.

The composition of the low-temperature steady state of the goldfish  $A_2$ -pigment and the regenerated  $A_2$ -bovine pigment have been determined as a function of irradiation wavelength (Tables I and II). Isorhodopsin makes up the

TABLE I  
COMPOSITION OF 77 K REGENERATED  $A_2$ -BOVINE  
PIGMENT STEADY STATE\*

$\lambda$	11- <i>Cis</i>	9- <i>Cis</i>	Photoproduct
<i>nm</i>			
488.0	13 (13-12)	54 (55-54)	33 (34-33)
514.5	11 (12-11)	58 (59-57)	30 (32-29)
530.9	8.6 (8.9-8.3)	64 (66-62)	27 (29-25)
568.2	—	87 (90-85)	13 (15-10)
676 and 488	42 (44-39)	46 (48-43)	13 (15-9)

\*The range of percent compositions found in two to five determinations is given in parentheses.

TABLE II  
COMPOSITION OF 77 K  $A_2$ -GOLDFISH PIGMENT  
STEADY STATE

$\lambda$	11- <i>Cis</i>	9- <i>Cis</i>	Photoproduct
<i>nm</i>			
488.0	17 (18-15)	45 (47-43)	39 (42-35)
514.5	15 (18-12)	55 (58-52)	30 (31-29)
530.9	17 (20-14)	57 (61-52)	26 (29-23)
568.2	—	82 (84-80)	18 (20-16)

majority of the  $A_2$ -pigment steady-state mixture for irradiation between 488 and 568 nm and the 11-*cis* pigment never makes up more than 17%. Accordingly, as the Raman probe wavelength is varied between 488 and 568 nm, the Raman spectrum of these pigments should reflect a large contribution from the 9-*cis* pigment and very little contribution from the 11-*cis* pigment. At 488 nm, where the 9-*cis* pigment and the photoproduct are present in nearly equal amounts, the Raman spectrum will still be dominated by the 9-*cis* species, since the 9-*cis* pigment is much more resonantly enhanced at this wavelength than the red-shifted photoproduct. These are exactly the results we have observed in our Raman studies on the  $A_2$ -pigments.

We can use the relative extinction coefficients of the low-temperature  $A_2$ -species and the compositions in Tables I and II to determine relative quantum yields,  $\phi_1/\phi_2$  and  $\phi_3/\phi_4$ , at each of these irradiation wavelengths. The individual quantum yields can then be determined by knowledge of  $\phi_1$  and measurement of  $\phi_2/\phi_3$ . For  $A_2$ -pigments,  $\phi_1$  has been found to be 0.64 and to be wavelength independent (27);  $\phi_1$  in  $A_1$ -pigments is 0.67 and also wavelength independent (28, 29). The  $A_2$ -quantum yield in reference 27 was measured at room temperature, and we assume that it is the same at 77 K. Such temperature-independent photochemistry is a well-documented phenomenon for  $A_1$ -rhodopsin (30).<sup>1</sup> The ratio  $\phi_2/\phi_3$  can be determined at low-temperature by a method similar to the one used by Suzuki and Callender (8). The 11-*cis* regenerated  $A_2$ -bovine pigment is irradiated with 488-nm light to produce a steady state rich in the photoproduct. Subsequently, 3 min of illumination with an expanded 676-nm laser beam (30 mW) converts some of the photoproduct to the 11-*cis* and 9-*cis* pigments. Under these conditions,  $\phi_2/\phi_3 = \Delta Rho/\Delta Iso$ , where  $\Delta Rho$  is the change in the composition of the 11-*cis* pigment and  $\Delta Iso$  is the change in the composition of the 9-*cis* pigment. The 676-nm wavelength is chosen to minimize backreaction from the 11-*cis* and 9-*cis* pigments and to prevent the production of a steady state. After this irradiation, the photoproduct still made up

<sup>1</sup>However, it should be noted that temperature-dependent all-*trans*  $\rightarrow$  13-*cis* photochemistry has been observed for the  $A_2$ -chromophore regenerated in bacteriorhodopsin (41).

13% of the mixture, and the value of  $\phi_2/\phi_3$  was found to be 3.37. Experiments in which the sample was irradiated with a 60 mW beam for 3 min left an average of only 5% bathorhodopsin in the low-temperature steady state, and the value of  $\phi_2/\phi_3$  was 3.33. We assumed that this value of  $\phi_2/\phi_3$ , measured in the regenerated A<sub>2</sub>-bovine pigment, is also correct for the A<sub>2</sub>-goldfish pigment and that  $\phi_2/\phi_3$  is wavelength independent.

The wavelength dependence of the quantum yields in Tables III and IV deserves comment. The ratios  $\phi_1/\phi_2$  and  $\phi_3/\phi_4$  are somewhat wavelength dependent in the regenerated A<sub>2</sub>-bovine pigment (Table III) but they do not appear to vary with wavelength for the A<sub>2</sub>-goldfish pigment (Table IV). This gives rise to wavelength-dependent values of  $\phi_2$ ,  $\phi_3$ , and  $\phi_4$  for just the A<sub>2</sub>-bovine pigment. Given the magnitude of the experimental error we do not believe that these measurements can be used to reliably address the presence or absence of wavelength dependence in the A<sub>2</sub>-photochemistry. A more detailed study of  $\phi_1/\phi_2$ ,  $\phi_3/\phi_4$ , and  $\phi_2/\phi_3$  vs. wavelength is needed to determine whether the trends observed here are significant. For comparison, it should be noted that the low-temperature steady-state measurements of  $\phi_4$  in A<sub>1</sub>-pigments by Suzuki and Callender (8) showed no wavelength dependence, whereas non-steady-state measurements have observed a significant wavelength dependence of  $\phi_4$  (30, 31).

## DISCUSSION

A<sub>2</sub>-visual pigments have many of the photochemical properties of the commonly studied A<sub>1</sub>-pigments. It has been shown previously that, like A<sub>1</sub>-rhodopsin, the room temperature quantum yield of A<sub>2</sub>-rhodopsin is large and wavelength independent (27–29). The A<sub>2</sub>-pigment forms a 77-K steady state composed of three intermediates. Also, the A<sub>2</sub>-photoproduct has enhanced hydrogen out-of-plane modes in the Raman spectrum which have similar intensity and frequency to those of the A<sub>1</sub>-photoproduct. This suggests that substitution of A<sub>2</sub>-retinal for A<sub>1</sub>-retinal does not qualitatively alter the conformational distortions imposed on the photoproduct by the protein.

However, the 77-K photostationary steady-state composition of the A<sub>2</sub>-pigment differs from that of the A<sub>1</sub>-pigment, and the regeneration experiments show that this

TABLE III  
QUANTUM YIELDS FOR REGENERATED A<sub>2</sub>-BOVINE PIGMENT\*

$\lambda$	$\phi_1/\phi_2$	$\phi_3/\phi_4$	$\phi_2$	$\phi_3$	$\phi_4$
<i>nm</i>					
488.0	1.6 ± 0.1	3.2 ± 0.2	0.41	0.12	0.04
514.5	1.9 ± 0.2	2.9 ± 0.2	0.34	0.10	0.04
530.9	3.2 ± 0.4	2.4 ± 0.3	0.20	0.06	0.03
568.2	—	2.5 ± 0.7	—	—	—

\* $\phi_2$  was calculated from  $\phi_1/\phi_2$  using  $\phi_1 = 0.64$ .  $\phi_3$  and  $\phi_4$  were then obtained using  $\phi_2/\phi_3 = 3.4$ .

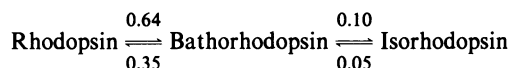
TABLE IV  
QUANTUM YIELDS FOR A<sub>2</sub>-GOLDFISH PIGMENT\*

$\lambda$	$\phi_1/\phi_2$	$\phi_3/\phi_4$	$\phi_2$	$\phi_3$	$\phi_4$
<i>nm</i>					
488.0	1.9 ± 0.3	1.9 ± 0.2	0.34	0.10	0.05
514.5	1.9 ± 0.7	2.2 ± 0.5	0.34	0.10	0.05
530.9	1.7 ± 0.4	2.0 ± 0.4	0.38	0.11	0.06
568.2	—	1.7 ± 0.3	—	—	—

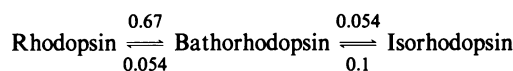
\* $\phi_2$  was calculated from  $\phi_1/\phi_2$  using  $\phi_1 = 0.64$ .  $\phi_3$  and  $\phi_4$  were then calculated using  $\phi_2/\phi_3 = 3.4$ .

is due to intrinsic photochemical differences between the A<sub>1</sub>- and A<sub>2</sub>-chromophores. There is a decrease in the quantum yield for 9-*cis* to all-*trans* isomerization at 77 K. We have also observed a decrease in this rate at room temperature (24). There is also an increase in the all-*trans* to 9-*cis* quantum yield and a small decrease in the all-*trans* to 11-*cis* quantum yield. Below, we compare the average quantum yields for the A<sub>2</sub>-pigments with previous results on the A<sub>1</sub>-bovine pigment (8).

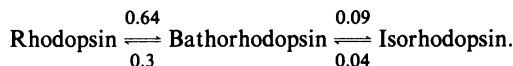
A<sub>2</sub>-goldfish pigment:



A<sub>1</sub>-bovine pigment:



A<sub>2</sub>-bovine pigment at 514.5 nm:



The mechanism responsible for the distinctive photochemistry of A<sub>2</sub>-visual pigments must arise from the extension of the  $\pi$ -electron system into the ionone ring. It is clear from the Raman spectra of these compounds that the extra double bond results in an increase in  $\pi$ -electron delocalization. A decrease in the frequency of the ethylenic stretching mode is observed; such a decrease implies that there is less bond alternation and a more delocalized electronic structure in A<sub>2</sub>-compounds. Also, in the Raman spectra of both the A<sub>2</sub>-retinals (32) and the A<sub>2</sub>-protonated Schiff bases (24), a new line appears at 1,172 cm<sup>-1</sup>. This line has been assigned to the C<sub>6</sub>—C<sub>7</sub> stretch in  $\beta$ -ionone (33). The enhancement of the C<sub>6</sub>—C<sub>7</sub> vibration in the spectra of A<sub>2</sub>-molecules is an indication that the  $\pi$ -electron transition induces bond-order changes that extend into the ionone ring. In A<sub>1</sub>-compounds, on the other hand, the C<sub>5</sub>=C<sub>6</sub> bond is believed to be relatively isolated from the rest of the conjugated chain by a 30–70° twist around the 6-*s-cis* single bond (34), and the C<sub>6</sub>—C<sub>7</sub> vibration does not appear in the Raman spectrum (33).

One possible explanation for the distinctive  $A_2$ -photochemistry is that the increase in delocalization in the  $A_2$ -chromophore alters the excited state barriers for isomerization and, hence, the isomerization quantum yields. Theoretical (35–37) and recent experimental (38) studies of retinyl-polyenes suggest that the central double bonds of the  $\pi$ -system undergo the largest bond length changes upon excitation. Addition of the double bond in the ring moves the center of the  $\pi$ -electron system towards the  $C_9=C_{10}$  bond. This model would predict, in agreement with our quantum yield measurements, that the all-*trans*  $A_2$ -chromophore has a lower excited state barrier for  $C_9=C_{10}$  isomerization and a higher barrier for  $C_{11}=C_{12}$  isomerization. However, such changes in excited state barriers, considered alone, would also predict an increase in the  $9$ -*cis*  $\rightarrow$  *trans* quantum yield. We observe a marked reduction in this quantum yield, indicating that other physical factors are contributing to the production of the unique photochemistry of the  $A_2$ -chromophore. Other data are consistent with our observation that *cis*  $\rightarrow$  *trans* and *trans*  $\rightarrow$  *cis* quantum yields do not necessarily increase or decrease in a simple way as the electron delocalization is altered. Freedman and Becker (39) have shown that protonation of  $A_1$ -retinal Schiff bases results in a large decrease in the  $9$ -*cis*  $\rightarrow$  *trans* quantum yield in methanol, while the *trans*  $\rightarrow$   $9$ -*cis* quantum yield is unaffected. Their work also shows that the  $11$ -*cis*  $\rightarrow$  *trans* quantum yield is unchanged by protonation.

The unique quantum yields of  $A_2$ -chromophores may be due to intramolecular steric effects that specifically stabilize the  $9$ -*cis* geometry. This steric effect might be a consequence of the increased  $\pi$ -electron delocalization in the  $A_2$ -chromophore. The  $A_2$ -retinal protonated Schiff base is likely to be more planar at the  $C_6-C_7$  bond and has a different ring conformation than the  $A_1$ -protonated Schiff base because of extension of the  $\pi$ -system. This change in the geometry will alter the interaction between the  $C_5$  methyl group and the polyene chain, which may indirectly alter the relative stabilities of the  $9$ -*cis* and  $9$ -*trans* isomers.

It is also possible that the stability of the  $9$ -*cis* isomer in the protein is due to a stabilizing intermolecular steric interaction between the protein and chromophore which is common to the goldfish and bovine opsins. The unique ionone ring geometry and twist angle at  $C_6-C_7$  in the  $A_2$ -chromophore may produce a  $9$ -*cis* chromophore conformation that is preferentially stabilized by the protein. Warshel and Barboy (40) have suggested that this type of intermolecular interaction may be an important factor in controlling photochemical quantum yields. It will now be important to measure the photochemical quantum yields of  $A_2$ -protonated Schiff bases in solution to determine whether the novel quantum yields observed here are due to an intermolecular or an intramolecular effect.

We thank F. Harosi for assisting us in the development of protocols for photoreceptor regenerations, I. Palings for helping to prepare bovine rod

outer segment samples, and Carola Heeremans for assistance with the  $A_2$ -retinal synthesis. We also thank W. Hubbell for the use of his darkroom facilities, P. Baldwin for helpful discussions, and J. Hearst for loaning us the Zeiss microscope.  $A_2$ -retinal samples used in initial phases of this work were generously provided by R. S. H. Liu.

This research was supported by the National Institutes of Health (EY-02051 and EY-00219); work carried out in Leiden was supported by the Netherlands Foundation for Chemical Research (SON) and the Netherlands Organization for the Advancement of Pure Research (ZWO). B. Barry was supported in part by a University of California Graduate Opportunity Fellowship.

Received for publication 20 March 1987 and in final form 26 June 1987.

## REFERENCES

1. Birge, R. R. 1981. Photophysics of light transduction in rhodopsin and bacteriorhodopsin. *Annu. Rev. Biophys. Bioeng.* 10:315–354.
2. Yoshizawa, T., and G. Wald. 1963. Pre-lumirhodopsin and the bleaching of visual pigments. *Nature (Lond.)* 197:1279–1286.
3. Oseroff, A. R., and R. H. Callender. 1974. Resonance Raman spectroscopy of rhodopsin in retinal disk membranes. *Biochemistry* 13:4243–4248.
4. Eyring, G., B. Curry, A. Broek, J. Lugtenburg, and R. Mathies. 1982. Assignment and interpretation of hydrogen out-of-plane vibrations in the resonance Raman spectra of rhodopsin and bathorhodopsin. *Biochemistry* 21:384–393.
5. Chabre, M. 1985. Trigger and amplification mechanisms in visual phototransduction. *Annu. Rev. Biophys. Biophys. Chem.* 14:331–360.
6. Stryer, L. 1986. Cyclic GMP cascade of vision. *Annu. Rev. Neurosci.* 9:87–119.
7. Yoshizawa, T. 1972. The behaviour of visual pigments at low temperatures. *Handb. Sens. Physiol.* 7/1:146–179.
8. Suzuki, T., and R. H. Callender. 1981. Primary photochemistry and photoisomerization of retinal at 77°K in cattle and squid rhodopsins. *Biophys. J.* 34:261–265.
9. Birge, R. R., and L. M. Hubbard. 1981. Molecular dynamics of *trans-cis* isomerization in bathorhodopsin. *Biophys. J.* 34:517–534.
10. Myers, A. B., and R. A. Mathies, 1987. Resonance Raman intensities: a probe of excited-state structure and dynamics. In *Biological Applications of Raman Spectroscopy*. Vol. 2. Resonance Raman Spectra of Polyenes and Aromatics. T. G. Spiro, editor. John Wiley & Sons, Inc., New York. 1–58.
11. Mathies, R. A., S. O. Smith, and I. Palings. 1987. Determination of retinal chromophore structure in rhodopsins. In *Biological Applications of Raman Spectroscopy*. Vol. 2. Resonance Raman Spectra of Polyenes and Aromatics. T. G. Spiro, editor. John Wiley & Sons, Inc., New York. 59–108.
12. Barry, B., and R. Mathies. 1982. Resonance Raman microscopy of rod and cone photoreceptors. *J. Cell Biol.* 94:479–482.
13. Barry, B., and R. A. Mathies. 1987. Raman microscope studies on the primary photochemistry of vertebrate visual pigments with absorption maxima from 430 to 502 nm. *Biochemistry* 26:59–64.
14. Forster, R. P., and J. V. Taggart. 1950. Use of isolated renal tubules for the examination of metabolic processes associated with active cellular transport. *J. Cell. Comp. Physiol.* 36:251–270.
15. Yoshikami, S., and G. N. Noll. 1982. Technique for introducing retinol analogs into the isolated retina. *Methods Enzymol.* 81/H:447–451.
16. Pepperberg, D. R. 1982. Generation of rhodopsin and “artificial” visual pigments in electrophysiologically active photoreceptors. *Methods Enzymol.* 81/H:452–459.
17. Harosi, F. I. 1984. *In vitro* regeneration of visual pigment in isolated photoreceptors. In *Photoreceptors*. A. Borsellino and L. Cervetto,

- editors. Plenum Press, New York. NATO Advanced Study Institute, Series A. 75:41-63.
18. Papermaster, D. S. 1982. Preparation of retinal rod outer segments. *Methods Enzymol.* 81/H:48-52.
  19. Schwanzara, S. A. 1967. The visual pigments of freshwater fishes. *Vision Res.* 7:121-148.
  20. Palings, I., J. A. Pardoën, E. van den Berg, C. Winkel, J. Lugtenburg, and R. A. Mathies. 1987. Assignment of fingerprint vibrations in the resonance Raman spectra of rhodopsin, isorhodopsin and bathorhodopsin: implications for chromophore structure and environment. *Biochemistry.* 26:2544-2556.
  21. Henbest, H. B., E. R. H. Jones, and T. C. Owen. 1955. Studies in the polyene series. Part LI. Conversion of vitamin A<sub>1</sub> into vitamin A<sub>2</sub>. *J. Chem. Soc. (Lond.).* 3:2765-2767.
  22. Tsukida, K., R. Masahara, and M. Ito. 1980. High-performance liquid chromatographic analysis of *cis-trans* stereoisomeric 3-dehydroretinals in the presence of retinal isomers. *J. Chromatog.* 192:395-401.
  23. Mathies, R., T. B. Freedman, and L. Stryer. 1977. Resonance Raman studies of the conformation of retinal in rhodopsin and isorhodopsin. *J. Mol. Biol.* 109:367-372.
  24. Barry, B. 1984. Ph.D. Thesis. University of California, Berkeley, CA.
  25. Braiman, M., and R. Mathies. 1982. Resonance Raman spectra of bacteriorhodopsin's primary photoproduct: evidence for a distorted 13-*cis* retinal chromophore. *Proc. Natl. Acad. Sci. USA.* 79:403-407.
  26. Eyring, G., B. Curry, R. Mathies, R. Fransen, I. Palings, and J. Lugtenburg. 1980. Interpretation of the resonance Raman spectrum of bathorhodopsin based on visual pigment analogues. *Biochemistry.* 19:2410-2418.
  27. Dartnall, H. J. A. 1958. The spectral variation of the relative photosensitivities of some visual pigments. In *Visual Problems of Colour*. Vol. 1. Natl. Phys. Lab. Symp. No. 8, London, H.M.S.O. 121-148.
  28. Schneider, E. E., C. F. Goodeve, and R. J. Lythgoe. 1939. The spectral variation of the photosensitivity of visual purple. *Proc. R. Soc. Edinb. Sect. A. (Math. Phys. Sci.).* 170:102-112.
  29. Dartnall, H. J. A. 1968. The photosensitivities of visual pigments in the presence of hydroxylamine. *Vision Res.* 8:339-358.
  30. Hurley, J. B., T. G. Ebrey, B. Honig, and M. Ottolenghi. 1977. Temperature and wavelength effects on the photochemistry of rhodopsin, isorhodopsin, bacteriorhodopsin and their photo-products. *Nature (Lond.).* 270:540-542.
  31. Schick, G. A., T. M. Cooper, R. A. Holloway, L. P. Murry, and R. R. Birge. 1987. Energy storage in the primary photochemical events of rhodopsin and isorhodopsin. *Biochemistry.* 26:2556-2562.
  32. Cookingham, R. E., A. Lewis, and A. T. Lemley. 1978. A vibrational analysis of rhodopsin and bacteriorhodopsin chromophore analogues: resonance Raman and infrared spectroscopy of chemically modified retinals and Schiff bases. *Biochemistry.* 17:4699-4711.
  33. Curry, B., I. Palings, A. D. Broek, J. A. Pardoën, J. Lugtenburg, and R. Mathies. 1985. Vibrational analysis of the retinal isomers. *Adv. Infrared Raman Spectrosc.* 12:115-178.
  34. Honig, B., B. Hudson, B. D. Sykes, and M. Karplus. 1971. Ring orientation in  $\beta$ -ionone and retinals. *Proc. Natl. Acad. Sci. USA.* 68:1289-1293.
  35. Kakitani, H., T. Kakitani, H. Rodman, B. Honig, and R. Callender. 1983. Correlation of vibrational frequencies with absorption maxima in polyenes, rhodopsin, bacteriorhodopsin, and retinal analogues. *J. Phys. Chem.* 87:3620-3628.
  36. Sanchez-Marin, J., and J. P. Malrieu. 1985. Spectroscopy and photochemistry of conjugated nonprotonated Schiff bases: application of an *ab initio* derived Heisenberg effective Hamiltonian. *J. Am. Chem. Soc.* 107:1985-1992.
  37. Warshel, A., and M. Karplus. 1974. Calculation of  $\pi\pi^*$  excited state conformations and vibronic structure of retinal and related molecules. *J. Am. Chem. Soc.* 96:5677-5689.
  38. Smith, S. O., M. S. Braiman, A. B. Myers, J. A. Pardoën, J. M. L. Courtin, C. Winkel, J. Lugtenburg, and R. A. Mathies. 1987. Vibrational analysis of the all-*trans* retinal chromophore in light-adapted bacteriorhodopsin. *J. Am. Chem. Soc.* 109:3108-3125.
  39. Freedman, K. A., and R. S. Becker. 1986. Comparative investigation of the photoisomerization of the protonated and unprotonated *n*-butylamine Schiff bases of 9-*cis*, 11-*cis*, 13-*cis* and all-*trans* retinals. *J. Am. Chem. Soc.* 108:1245-1251.
  40. Warshel, A., and N. Barboy. 1982. Energy storage and reaction pathways in the first step of the vision process. *J. Am. Chem. Soc.* 104:1469-1476.
  41. Iwasa, T., F. Tokunaga, T. G. Ebrey, and T. Yoshizawa. 1981. The photoreactions and photosensitivity of 3,4-dehydrobacteriorhodopsin at low temperatures. *Photochem. Photobiol.* 33:547-557.